

# Remote inventory and inspection of the truss bridge elements and connections using STS and UAV

P. Olaszek<sup>1</sup>, E. Maciejewski<sup>2</sup>, A. Rakoczy<sup>2</sup>, R. Cabral<sup>3</sup>, R. Santos<sup>4</sup>, D. Ribeiro<sup>4</sup>

<sup>1</sup>Road and Bridge Research Institute,  
ul. Instytutowa 1, 03-302, Warsaw, Poland  
[polaszek@ibdim.edu.pl](mailto:polaszek@ibdim.edu.pl)

<sup>2</sup>Faculty of Civil Engineering, Warsaw University of Technology  
al. Armii Ludowej 16, Warsaw, Poland  
[edgar.maciejewski.stud@pw.edu.pl](mailto:edgar.maciejewski.stud@pw.edu.pl), [Anna.Rakoczy@pw.edu.pl](mailto:Anna.Rakoczy@pw.edu.pl)

<sup>3</sup>CONSTRUCT, Department of Civil Engineering, University of Porto  
R. Dr. Roberto Frias s/n, 4200-465 Porto, Portugal  
[up201609762@edu.fe.up.pt](mailto:up201609762@edu.fe.up.pt)

<sup>4</sup>CONSTRUCT, Department of Civil Engineering, Polytechnic of Porto  
R. Dr. António Bernardino de Almeida 431, 4249-015 Porto, Portugal  
[rps@isep.ipp.pt](mailto:rps@isep.ipp.pt), [drr@isep.ipp.pt](mailto:drr@isep.ipp.pt)

**Abstract.** The traditional visual inspections, along with the remote Structural Health Monitoring (SHM) methods are very valuable tools to keep the existing bridges safely in service. In the case of old structures with incomplete documentation, verification of dimensions is also an essential aspect. Traditional on-foot or on-boat visual inspections have many limiting factors. For large or tall structures, there is little to no possibility of visually inspecting the entire structure without using lifts or other heavy machinery. This paper presents an attempt to use a Scanning Total Station (STS) for the inspection and inventory of the dimensions of a truss railway bridge over the largest river in Poland. Measurements were conducted using two methods: the direct method with the use of a total station and the use of advanced geometric analyses of the collected point cloud. The field tests on the bridge were preceded by tests in the laboratory, where the accuracy of the method was assessed. During the tests on the bridge, a deviation from the actual geometry of the selected truss connection in relation to the old documentation was detected. The credibility and scale of this deviation throughout the bridge span were confirmed by Unmanned Aerial Vehicle (UAV) inspections.

**Keywords:** visual inspections, Scanning Total Station, Unmanned Aerial Vehicle.

## 1 Introduction

The increasing number of old and deteriorated bridge structures in the world has only highlighted the importance of their inspection and maintenance. The traditional visual inspections along with the remote Structural Health Monitoring (SHM) methods are very valuable tools to keep the bridges safely in service. In the case of old structures with incomplete documentation, verification of dimensions is also an essential aspect. Traditional on-foot or on-boat visual inspections have many limiting factors. For large or tall structures, there is little to no possibility of visually inspecting the entire structure without using lifts or other heavy machinery.

Many researchers and industrial centers around the world are working on the use of modern techniques for remote inspection of bridges [1]. Nepomuceno et al. [2] present a potential schema for remote visual inspections. They emphasize that the risk to inspectors' health and safety would be reduced when they are not required to be on-site. On-site photographers (with the use of a 360° camera) are expected to spend less time on-site than a traditional inspector. Galdelli et al. [3] and Ribeiro et al. [4] presented a remote visual inspection system for bridge predictive maintenance and proposed, integrating robotics with vision solutions. Nguyen et al. [5] show developing a Building Information Modelling (BIM)-based Mixed Reality (MR) application to enhance and facilitate the process of managing bridge inspection and maintenance tasks remotely from the office.

This paper presents an attempt to use a Scanning Total Station (STS) and photogrammetric documentation recorded with the use of an Unmanned Aerial Vehicle (UAV) for the inspection and inventory of the dimensions of a truss railway bridge over the Vistula River in Poland.

## **2 STS applications for bridge inspection and inventory**

### **Surveying equipment**

To create the geometry of the selected bridge part a STS was used. This device is capable of conducting precise reflector-less measurements as well as the ability to create point clouds by laser scanning. The basic parameters of this device are: angular accuracy equalled 1", distance measurement accuracy onto prism 1 mm + 1.5 ppm and any surface 2 mm + 2 ppm, scanning with 1000 Hz mode – range to 300 m with range noise 1.0 mm at 50 m and scanning with 1 Hz mode – range to 1000 m with range noise 0.6 mm at 50 m (Grimm [6]). The instrument can be used in various applications of the bridge's SHM. For example Omidalizarandi et al. [7] and Erhart et al. [8] present applications for vision-based displacement and vibration analysis of bridges. Sanchez-Cuevas et al. [9] present the application of the STS to assist UAVs in inspection, which requires physical contact between the aerial platform and the bridge surfaces.

### **Laboratory tests to assess the accuracy of the method**

Two laboratory tests were conducted to assess the accuracy of the measurement method in different environmental conditions. In both tests, the measured object was a steel bar on a balcony, as seen in Figure 1. This was performed to simulate the conditions that could be present at the bridge site — the vertical distance between the station and measured elements. The tests aimed to measure the dimensions of the beam using reflector-less measurements and point cloud scanning, and then compare the results with the known dimensions of the beam.



Figure 1. Laboratory tests; from the left: scan area as indicated on the display; from the right: Scanning Total Station during field survey.

The first test (No. 1) was designed to analyze the influence of atypical geometry on the measurements. The beam had a rectangular cross-section with bent and smooth edges. This test has revealed several problems with manual measurements. Firstly, the location of the measured object has made it very difficult to aim at the target points correctly. The bent edges of the beam had a substantial effect on the accuracy. It is assumed that this is primarily due to how a bent smooth edge reflects the laser beam. Difficulty in target acquisition of an elevated target was also noticed. The second test (No. 2) was done on a beam with a rectangular cross-section and sharp edges. This test has confirmed that the shape of the measured object has a substantial influence on the measurements. To mitigate the effect of the shape of the beam on the results, five points were measured on the opposite sides of the beam. Then a plane was fitted to each set of points, and the distance between the two parallel

planes was calculated. This approach is only applicable to symmetrical objects with at least two parallel faces. Additionally, in both tests, laser scanning was done. The scan area of one of the scans can be seen in Figure 1. The STS can capture point clouds from several stations and combine them into one during surveying on the built-in software. This allows for on-site verification of obtained scans. Combined point clouds captured from at least two measuring stations were created. The point clouds were then used to obtain the dimensions of the beams in both tests.

### **Applied algorithms for determining dimensions from the point cloud**

Point cloud data obtained in controlled (as shown in Figure 2) consisted of the balcony, the beam itself, and part of a wall behind. Several cloud processing operations were conducted to obtain the desired dimension from the point cloud that contained almost one million points. The cloud was cropped to narrow down the beam itself. Then two M-estimator Sample Consensus (M-SAC) based algorithms were introduced to separate opposite faces of the beam. The M-SAC algorithm is a version of the Random Sample Consensus RANSAC algorithm – Pleasamai & Chaiyasarn [10], which has been used in similar applications for many years.

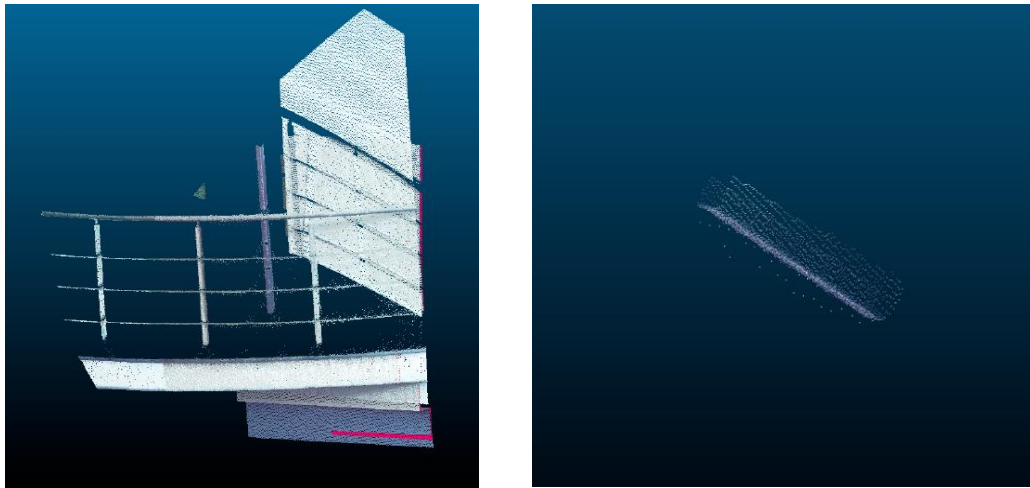


Figure 2. The processing of the point cloud data; from the left: the final point cloud in test No. 1; from the right: the region of the point cloud from the test No. 1 used in calculations.

The scanned object has a rectangular cross-section; therefore it can be separated into two sets of parallel planes. The scanned steel bar was only visible from the front and two sides. The sides are then considered as two parallel planes. The distance between them is the dimension to be measured. The approach was to find the best-fitting planes for two opposite surfaces of the cross-section. Firstly, the cropped portion of the point cloud was cleaned using a Statistical Outlier Removal (SOR) filter. Then the resulting cloud was treated with two versions of the parallel plane fitting M-SAC algorithm. This method of fitting a data set to a mathematical model by selecting a random small region of interest, obtaining an initial solution, and expanding it is well suited to point cloud processing. This version of the algorithm uses the M-estimator function to fit data to a geometric model of a plane. The first approach was to find the best-fitting plane using a normal vector perpendicular to one of the sides of the object. Then this vector is used to find the second plane. Because of the nature of the algorithm and tolerances, these planes are not perfectly parallel. One of the planes is then shifted to match the other's normal vector, making the resulting planes parallel. The distance between them is found. This operation is repeated starting from the other side of the beam, and the distance is averaged. Another approach was to use M-SAC to fit a plane on each side of the beam. Then for each of the two sides, the inlier points, which are the points located within a tolerated distance from the found plane, are extracted from the point cloud. These (close to the plane but not exactly on it) points are used to fit two parallel planes different from the ones found by M-SAC. This approach used the same fitting function as the calculations used to fit parallel planes with points from manual measurements used in the second test (No. 2). Therefore, there is a variance between each run of the algorithm. To obtain the best results, both approaches were iterated one thousand times. The mean distance between the planes was calculated, and an

average was taken for the whole fitting process. The number of iterations was chosen by observing the convergence of the results and the number of iterations that failed to find a suitable fit. Considerable significance was placed on finding suitable fitting parameters. The tolerances of the maximum distance from the fitted plane for inlier points were set to the resolution of the scan, which was 0.002 m. The angular tolerance for finding the normal vectors was set to 0.02 deg. Preliminary data processing was performed in CloudCompare [11] and basic algorithms were implemented in MatLab [12].

### Small-scale elements measurement results

It has been noticed that the smooth edges of the beam in test No. 1 could incorrectly reflect the laser beam of the measuring device, thus impacting its performance. The Wave Form Digitizing (WFD) technology used in the measurement device is supposed to mitigate inaccuracies caused by laser dot size. However, in test No. 1, it was not possible to achieve a satisfactory accuracy of manual measurements. This could be caused by the steep horizontal and vertical angle of the measured object. Such conditions could be present on-site during the survey.

Table 1. Comparison of different measurement methods and achieved deviations

Method	Obtained dimension [mm]	Difference [mm]	Deviation [%]
Direct measurements (two stations)	42.4	2.4	6.0%
Point cloud data mean distance (approaches 1 and 2)	43.5	3.5	8.8%
Plane fitting	44.2	4.2	10.5%
Caliper	40.0	0.0	-

Three different methods were used to determine the dimension of the rectangular beam in test two (No. 2). The resulting dimensions obtained were then compared to measurements made with a caliper. The relative deviation was calculated as the difference divided by the reference measurement. These results are collected in Table 1. Direct measurements taken from two surveying stations in test No. 2 have achieved a satisfactory relative accuracy of six percent for a dimension of 40 mm. That, as opposed to test No.1, confirms that the shape of the edges of the measured object considerably influences the measurements. The point cloud data obtained during laboratory tests has shown similar accuracy. The average dimension obtained achieved a relative deviation of less than nine percent. That has confirmed that the STS is capable of creating accurate point cloud data, as well as the ability to merge several point clouds into one data set. Finally, a way of increasing the accuracy of manual measurements was introduced. The plane-fitting approach uses a set of points on the surface to calculate a plane model of the side of the object. This approach was developed to mitigate the problems of smooth edges, as seen in test No. 1. It is capable of mitigating such problems with a relative deviation of around ten percent. It must be noted that the accuracy of manual measurements is largely dependent on the human operator and thus might vary significantly between surveys. The point cloud and data are independent of the human factor and can be used even in the most challenging surveys. It should be added that the measurements were performed for small cross-sections, which resulted in significant relative deviations. Overall, the laboratory tests (resulting in absolute deviations) have shown that the device and methods achieved adequate accuracy for engineering applications.

## 3 The field tests on the bridge

### 3.1 Truss railway bridge

Gdański Railway Bridge in Warsaw is a multi-span, steel truss bridge over the Vistula River in Poland. The bridge has two separate structures for each of the railway lines. One of these structures was constructed in the 1980s and was renovated in 2015; the second was rebuilt in 2015. Each of the structures consists of eight spans of over 60 meters in length and two smaller spans on each end. The bridge and the analysed connection, as seen from the riverbank is shown in Figure 3.

### 3.2 The measured connection

For the experiment, a main structural connection of the truss, shown in Figure 4, was chosen. It is a W-type asymmetrical connection, joining one vertical member and two diagonal members with the lower chord of the truss. The members are connected by a gusset plate and are joined using rivets. Each of the three riveted connections is unique in the number and position of the connectors. This connection was selected for Remote inventory and inspection using STS and UAV since it was designated as repaired in the post-renovation documentation. In addition, the location of the connection provided easy access to the measurements from the sidewalk under the bridge.

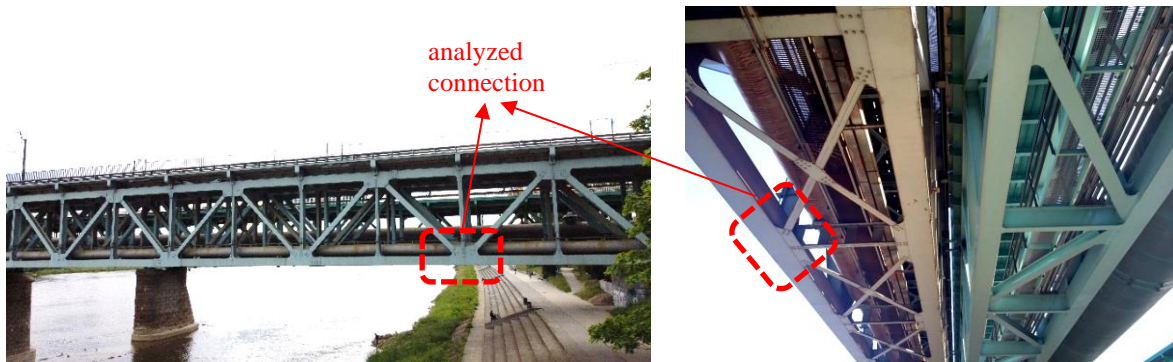


Figure 3. The view of the bridge



Figure 4. Photographs of the analyzed connection; from the left: taken from a UAV; from the right: taken from STS.

### 3.3 The results of measurements

The W-type connection previously highlighted was measured using STS and UAV systems to perform remote inventory and inspection. The survey aimed to compare the available digital documentation of the selected connection with survey data. The only available documentation was made during renovation work. No original design documents could be found.

The STS was conducted to create a combined point cloud of the whole connection. Additionally, reflectorless measurements were also performed. The combined point cloud consisted of over three million points. It was then cropped and cleaned to only include the main parts of the connection. Overall, over one million points were included in the processed data set.

The UAV was used to acquire 646 images from the span studied for creating a point cloud using photogrammetry. The system allowed to reconstruct the façade of the steel truss bridge as depicted in Figure 5. The technique showed a few limitations related to an insufficient number of images of the area resulting in voids in the point cloud.





Figure 5. Façade of steel truss bridge

Finally, the resulting point cloud from both systems required some processing techniques to be able to compare to the available 2D drawings. Flattening algorithms were used. Firstly, a best-fitting plane was found, then the data set points were all projected onto the plane as shown in Figure 6. The projected points were then traced to create a contour of the flattened point cloud. The final comparison of the STS and UAV system can be seen in Figure 6 and Figure 7, respectively.

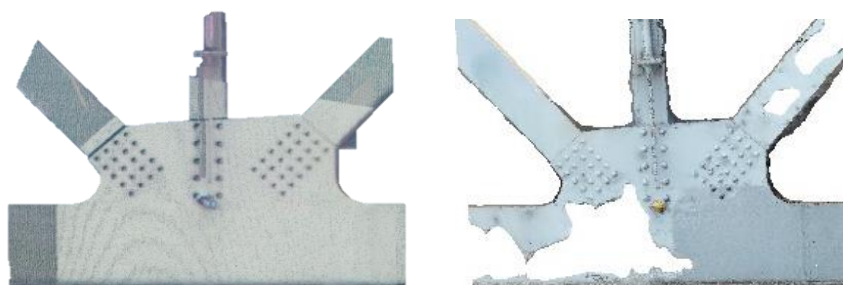


Figure 6. Point cloud of the analyzed connection projected onto the 2D plane; from the left: STS system; from the right: UAV system

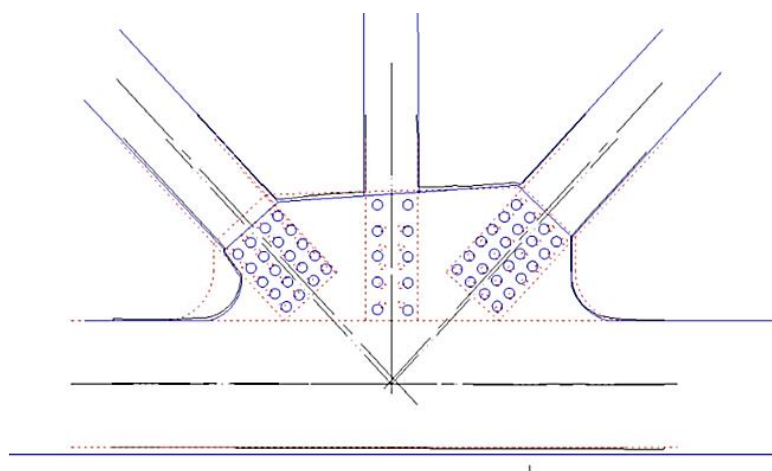


Figure 7. Geometry verification: STS point cloud contour (black solid line), UAV point cloud contour (blue solid line) and documentation drawing (red dotted line).

Several discrepancies between the documentation and the observed structure were found during surveying. For example, the left diagonal member has been found to be connected with less material than indicated in the drawings. The shape of the gusset plate on the left side has been found to be altered. It was found that the rows of rivets connecting the vertical member are spaced horizontally with a 69% and 61% relative deviation and vertically at a 41% and 37% relative deviation (calculated in the same way as in laboratory tests) for the STS and UAV system respectively. The rest of the dimensions, such as the member width, the height of the lower chord, or the spacing of the diagonal member's connectors, were all measured to be within a 10% relative deviation compared to the documentation. Such discrepancies might be the result of changes made during the construction process or a product of renovation works.

## 4 Conclusions

Laboratory and field tests confirmed the usefulness of STS and UAV for remote measurements and inventory of bridge structures. Based on laboratory tests implementing STS, it must be noted that the accuracy of manual measurements is largely dependent on the human operator and thus might vary significantly between surveys. The point cloud and data are independent of the human factor and can be used even in the most challenging surveys. Overall, the laboratory tests have shown that the device and methods achieved adequate accuracy for engineering applications. Based on field tests on the bridge it was confirmed that STS and UAV are effective at finding small but potentially significant deviation of bridge geometry in the investigated connection without the need to engage costly and disruptive machinery to aid on-foot inspections.

**Acknowledgments.** This work is framed on the project “Intelligent structural condition assessment of existing steel railway bridges” financed by the bilateral agreement FCT-NAWA (2022-23). The research covered in this article related to use of STS is performed under Edgar Maciejewski's (second author) Master Thesis. The authors extend gratitude to the personnel from the Railway Lines Unit in Warsaw of PKP Polskie Koleje Państwowe S.A. who helped with the project implementation and Natalia Kur from Road and Bridge Research Institute for help with the STS measurements. Additionally, thank the financial support by the doctoral grant UI/BD/150970/2021 - Portuguese Science Foundation, FCT/MCTES.

**Authorship statement.** The authors hereby confirm that they are the sole liable persons responsible for the authorship of this work and that all material that has been herein included as part of the present paper is either the property (and authorship) of the authors or has the permission of the owners to be included here.

## References

- [1] R. Cabral *et al.*, ‘Railway Bridge Geometry Assessment Supported by Cutting-Edge Reality Capture Technologies and 3D As-Designed Models’, *Infrastructures*, vol. 8, no. 7, p. 114, Jul. 2023, doi: 10.3390/infrastructures8070114.
- [2] D. T. Nepomuceno, J. Bennetts, M. Pregolato, T. Tryfonas, and P. J. Vardanega, ‘Development of a schema for the remote inspection of bridges’, *Proceedings of the Institution of Civil Engineers - Bridge Engineering*, pp. 1–16, Nov. 2022, doi: 10.1680/jbren.22.00027.
- [3] A. Galdelli *et al.*, ‘A Novel Remote Visual Inspection System for Bridge Predictive Maintenance’, *Remote Sensing*, vol. 14, no. 9, Art. no. 9, Jan. 2022, doi: 10.3390/rs14092248.
- [4] D. Ribeiro, R. Santos, R. Cabral, and R. Caçada, ‘Remote Inspection and Monitoring of Civil Engineering Structures Based on Unmanned Aerial Vehicles’, in *Advances on Testing and Experimentation in Civil Engineering*, C. Chastre, J. Neves, D. Ribeiro, M. G. Neves, and P. Faria, Eds., in Springer Tracts in Civil Engineering. Cham: Springer International Publishing, 2023, pp. 123–144. doi: 10.1007/978-3-031-23888-8\_6.
- [5] D.-C. Nguyen, T.-Q. Nguyen, R. Jin, C.-H. Jeon, and C.-S. Shim, ‘BIM-based mixed-reality application for bridge inspection and maintenance’, *Construction Innovation*, vol. 22, no. 3, pp. 487–503, Jan. 2021, doi: 10.1108/CI-04-2021-0069.
- [6] D. E. Grimm, ‘Leica Nova MS50: The World’s First MultiStation’, *GeoInformatics*, vol. 16, no. 7, p. 22, 2013.
- [7] M. Omidalizarandi, B. Kargoll, J.-A. Paffenholz, and I. Neumann, ‘Accurate vision-based displacement and vibration analysis of bridge structures by means of an image-assisted total station’, *Advances in Mechanical Engineering*, vol. 10, no. 6, p. 168781401878005, Jun. 2018, doi: 10.1177/1687814018780052.
- [8] M. Ehrhart, S. Kalenjuk, and W. Lienhart, ‘Monitoring of bridge vibrations with image-assisted total stations’.
- [9] P. J. Sanchez-Cuevas, P. Ramon-Soria, B. Arrue, A. Ollero, and G. Heredia, ‘Robotic System for Inspection by Contact of Bridge Beams Using UAVs’, *Sensors*, vol. 19, no. 2, Art. no. 2, Jan. 2019, doi: 10.3390/s19020305.
- [10] K. Pleansamai and K. Chaiyasarn, ‘M-estimator sample consensus planar extraction from image-based 3d point cloud for building information modelling’, *GEOMATE*, vol. 17, no. 63, Nov. 2019, doi: 10.21660/2019.63.09667.
- [11] ‘CloudCompare - home’. <https://www.cloudcompare.org/main.html> (accessed Aug. 10, 2023).
- [12] ‘MATLAB - MathWorks’. <https://www.mathworks.com/products/matlab.html> (accessed Oct. 08, 2017).